

Wavelet Based Classification for Cancer Diagnosis

Bhadra Mani¹, C. Raghavendra Rao², P. Anantha Lakshmi^{3*}, Asima Pradhan⁴ and Prasanta K. Panigrahi⁵

Abstract — We make use of discrete wavelets to extract distinguishing features between normal and cancerous human breast tissue fluorescence spectra. These are then used in conjunction with discriminant analysis for the purpose of reliable tissue differentiation. The wavelet coefficients at different levels of decomposition, representing intensity variations at different scales, are selected as feature vectors wherein the multiresolution and localization properties of wavelets are optimally exploited for identifying features. This wavelet based approach, when combined with the sensitive polarized fluorescence data, yielded statistically reliable characterization of tissue types for diagnostic purpose. Analysis of a number of data sets belonging to both perpendicular and parallel polarized spectra have led to key distinctions between cancerous, benign and normal tissues.

Key words — Cancer diagnostics, discrete wavelet transform, high-pass coefficients, linear discriminant analysis.

I. INTRODUCTION

In recent times, the rapid progress in the field of lasers, fiber optics, and mathematical modeling have led to the emergence

of computer aided diagnostics (CAD)[1]. Amongst various optical methods for tissue diagnostics, fluorescence spectroscopy [2] is one of the preferred choices, due to its sensitivity to molecular environment and biochemical changes that take place during the progress of disease. A number of key fluorophores have been identified, which show marked differences in behavior, in cancerous and normal tissues. Significant progress in cancer diagnosis using tissue fluorescence has been achieved, since the early work of Alfano and coworkers, on the tumor detection in rat tissues [3,4,5]. Many of these native fluorophores used for laser-induced fluorescence need to be excited through ultraviolet light; for example UV excited fluorescence probes NADH, tryptophan and tyrosine. In this work, we consider the fluorescence due to fluorophores like flavin and porphyrin, which can be excited by visible light, thereby avoiding the potentially damaging effect of UV light.

A number of techniques, separable into two broad categories, viz., statistical analysis [6,7] and physical modeling [8], have been employed for the study of the spectral data. In this paper, we make use of wavelet transform [9] for extracting reliable features for tissue discrimination. It is worth noting that, in recent times, wavelet transform has emerged as a powerful tool for data analysis. The ability of the wavelets to provide multiresolution, in addition to their localization properties, makes them ideal tool for studying data sets having different structures. In the present context, wavelet analysis enables us to separate out the spectral fluctuations at various scales; in the process, pinpointing characteristic differences in the spectra of cancerous, benign and normal human tissues. Furthermore, it also leads to a much more transparent dimensional reduction of the data set, which is an added advantage when dealing with large data sets. Here, discrete wavelet transform (DWT) has been used and the finite extension of the wavelet basis is employed to effectively capture collective behavior and sharp changes and localize them. Furthermore, their effect at various scales can also be probed making use of the mathematical microscopic nature of the wavelets.

An important aspect to be noted is that wavelets can be designed to have a number of useful properties, like being blind to regular structures; which can be particularly useful for the statistical modeling of the spectral fluctuations, since the random fluctuations from their correlated counterparts can be separated through these wavelets. As has been shown recently, wavelets are ideal for handling irregular data series [10,11,12]. Given the observed signal, $y(t) = f(t) + e(t)$, where $f(t)$ is the signal and $e(t)$ the noise, Donoho and co-workers have shown in the above references the usefulness of the wavelets in

¹ School of Physics, University of Hyderabad, Hyderabad – 500 046, India, e-mail: bhadramani@yahoo.com

² Department of Mathematics and Statistics, School of Mathematics and Computer/Info. Sciences, University of Hyderabad, Hyderabad – 500 046, India, e-mail: errsm@uohyd.ernet.in

³ School of Physics, University of Hyderabad, Hyderabad – 500 046, India e-mail: palsp@uohyd.ernet.in

⁴ Department of Physics, Indian Institute of Technology, Kanpur – 208 016, India, e-mail: asima@iitk.ac.in

⁵ Physical Research Laboratory, Ahmedabad – 380 009, India, e-mail: prasanta@prl.ernet.in

*Corresponding author.

extracting $f(t)$, when the noise is below a certain threshold and the signal variation is well above it. It must be emphasized that, traditional methods like local smoothing for extracting the signal will prove to be ineffective for irregular signals.

In our analysis below, DWT is being used for finding the appropriate features. It is combined with linear discriminant analysis (LDA) for tissue characterization. Classification function is obtained using LDA, which is a commonly used technique for classification [13].

The paper is organized as follows. In Section II and III, we first give an outline of the DWT and LDA respectively. After a brief description of the materials and methods in Section IV, we proceed to analyze, in detail, the results of the wavelet transform of the fluorescence data in Section V. Conclusions and possible extensions of the work are presented in Section VI. We conclude in Section VI, after pointing out directions of further research where wavelet transform along with other classification methods like neural networks may find profitable application.

II. WAVELET TRANSFORM

For long, Fourier transform remained as the most popular technique for analysis of signals. It was further improved with the advent of windowed Fourier transform, in which a window is used to localize frequencies. The window is a time function whose values are non zero only in a finite time interval. Windowed Fourier transform has its own limitations such as fixed size of the window resulting in problems of resolution. Therefore, selecting a small window to look for high frequencies could result in loss of information at low frequencies and vice versa. Wavelet transform circumvents this problem by having variable window sizes, commensurate with the frequency being considered [14,15].

Of late, wavelet methods have become a wide spread tool in many research domains in general and signal processing in particular. Wavelets provide sets of basis functions, which are complete and orthonormal. Unlike Fourier analysis they have both spatial & frequency localization, being most suitable for extracting hidden information/pattern out of sharply varying and non periodic signals. Analogous to Fourier series, discrete Fourier transform and integral Fourier transform in Fourier domain, one has wavelet series, discrete wavelet transform and continuous wavelet transform respectively in wavelet domain. In the present context only discrete wavelet transform is used

Wavelets provide a complete orthonormal basis set, where one starts from two members—father wavelet and mother wavelet and producing the others through translation and scaling. The father and mother wavelets, denoted by ϕ and ψ respectively, are square integrable, mutually orthogonal functions satisfying the following relations.

$$\int_{-\infty}^{+\infty} |\psi(t)|^2 dt = A \quad ,$$

$$\int_{-\infty}^{+\infty} \psi(t) dt = 0$$

$$\int_{-\infty}^{+\infty} |\phi(t)|^2 dt = B \quad ,$$

$$\int_{-\infty}^{+\infty} \phi(t) dt = 1$$

‘A’ and ‘B’ are constants. The daughter wavelets and scaling function at different scales are given by

$$\psi_{j,k} = 2^{j/2} \psi(2^j t - k)$$

$$\phi_{j,k} = 2^{j/2} \phi(2^j t - k)$$

Where, k is the translation parameter; j is the scaling parameter in the dyadic basis. The factor $2^{j/2}$ is there for normalization; is worth observing that the translation at each scale is commensurate with the same. Explicitly, at scale j , the translation unit is $2^{-j/2}k$.

All wavelet basis functions satisfy the dilation equation, also known as multiresolution analysis (MRA)

$$\phi(t) = \sum_n h(n) \sqrt{2} \phi(2t - n)$$

and

$$\psi(t) = \sum_n \tilde{h}(n) \sqrt{2} \psi(2t - n)$$

Physically, it means that, scaling function and wavelet at a given scale, can be constructed from the linear superposition of scaling function alone, at a higher scale. The initial scale in a given basis set is arbitrary, to be chosen keeping the application in mind. For the Haar wavelet

$$h(0) = h(1) = \frac{1}{\sqrt{2}}$$

$$\text{and } \tilde{h}(0) = -\tilde{h}(1) = \frac{1}{\sqrt{2}}$$

It is clear that the Haar basis is special, since it is the only wavelet, which is symmetric and compactly supported. Any finite energy signal $f(t) \in L^2\{R\}$ can be expanded as

$$f(t) = \sum_{k=-\infty}^{\infty} c_{j,k} \phi_{j,k}(t) + \sum_{k=-\infty}^{\infty} \sum_{i=j}^{\infty} d_{i,k} \psi_{i,k}(t)$$

The coefficients in the above expansion are given by the projections

$$c_{j,k} = \langle f(t), \phi_{j,k}(t)^* \rangle = \int_{-\infty}^{\infty} f(t) \phi(j,k)^* dt$$

$$d_{j,k} = \langle f(t), \psi_{j,k}(t)^* \rangle = \int_{-\infty}^{\infty} f(t) \psi(j,k)^* dt$$

If the scaling function is well behaved, then at a sufficiently high scale, the scaling function resembles a Dirac delta function and the corresponding coefficients simply sample the function. In other words, at high enough resolution, samples of the signal are very close to the scaling coefficients; this satisfies Shannon's sampling theorem. We shall be using discrete wavelet basis sets, in which case $c_{j,k}$'s and $d_{j,k}$'s are the DWT of the data. Using these coefficients one can also reconstruct the original data set. The wavelet coefficients at various scales can be appropriately thresholded to remove noise and smoothen the data, if so desired.

III. LINEAR DISCRIMINANT ANALYSIS

Statistical methods designed to elicit information from data sets which include simultaneous measurements on many variables are called multivariate data analysis techniques [16]. The objectives of the multivariate data analysis may be any one of the following (i) Data reduction (ii) Grouping (iii) Correlations (iv) Prediction (v) Testing of hypotheses.

In particular, discriminant analysis is a multivariate technique for classifying a given object into one of the pre-defined groups. The linear discriminant analysis aims at consolidating the features linearly and discriminating the objects.

A brief description of the discriminant analysis for multivariate normal populations is given in the following.

Let $f_1(x)$ and $f_2(x)$ be multivariate normal densities with mean vectors μ_1 and μ_2 and variance-covariance matrix Σ_1 and Σ_2 respectively for the populations π_1 and π_2 . We further assume that both are normal populations with equal variance-covariance matrices i.e. $\Sigma_1 = \Sigma_2 = \Sigma$. The corresponding joint densities $f_i(x)$ of $X' = [X_1, X_2, X_3, \dots, X_p]$ for these two populations are given by

$$f_i(x) = \frac{1}{(2\pi^{p/2}) |\Sigma|^{1/2}} \exp \left[-\frac{1}{2} (x - \mu_i)' \Sigma^{-1} (x - \mu_i) \right]$$

Let $C(2|1)$, $C(1|2)$ be the cost of misclassification and P_1, P_2 be the prior probabilities of π_1 and π_2 respectively, where $P_1 + P_2 = 1$. The minimum expected cost of misclassification regions are

$$(4)$$

$$R_1 : \{x : \exp \left[-\frac{1}{2} (x - \mu_1)' \Sigma^{-1} (x - \mu_1) + \frac{1}{2} (x - \mu_2)' \Sigma^{-1} (x - \mu_2) \right] \geq \left(\frac{c(1|2)}{c(2|1)} \right) \left(\frac{P_1}{P_2} \right) \}$$

$$R_2 : \{x : \exp \left[-\frac{1}{2} (x - \mu_1)' \Sigma^{-1} (x - \mu_1) + \frac{1}{2} (x - \mu_2)' \Sigma^{-1} (x - \mu_2) \right] < \left(\frac{c(1|2)}{c(2|1)} \right) \left(\frac{P_1}{P_2} \right) \}$$

$$\text{For } \left(\frac{c(1|2)}{c(2|1)} \right) \left(\frac{P_1}{P_2} \right) = 1$$

$$R_1 : \left[(\mu_1 - \mu_2)' \Sigma^{-1} x - \frac{1}{2} (\mu_1 - \mu_2)' \Sigma^{-1} (\mu_1 + \mu_2) \right] \geq 0$$

$$R_2 : \left[(\mu_1 - \mu_2)' \Sigma^{-1} x - \frac{1}{2} (\mu_1 - \mu_2)' \Sigma^{-1} (\mu_1 + \mu_2) \right] < 0$$

In general, for multivariate populations, one develops a quadratic score function for each and every population given by the expression (8)

$$S_i(x) = \frac{1}{2} \ln(|\Sigma_i|) - \frac{1}{2} (x - \mu_i)' \Sigma_i^{-1} (x - \mu_i) + \ln(p_i) \quad (8)$$

The object will be classified into that population for which the score function is minimum.

IV. MATERIALS AND METHOD

The samples were excited with linearly polarized 488 nm wavelength of an Ar-ion laser (Spectra Physics 165, 5 W). The linearly polarized light was focused on the front surface of the tissue samples and fluorescent light was collected in the right angle geometry through an analyzer, whose optic axis was set parallel or perpendicular to the optic axis of the input polarizer. The fluorescence was recorded using triplemate monochromator (SPEX-1877E) and PMT (RCA C-31 034). Further details regarding the experimental setup can be found in [17]. Fluorescence spectra of 29 malignant and benign tumors with their normal counterparts were analyzed by the wavelet transform and classification is done using above mentioned method. The benign tumors studied were of two types; pericanalicular and intracanalicular, based on their pathological and morphological differences [18].

V. RESULTS AND DISCUSSION

In the following analysis, the physically transparent Haar basis set is used. The fluorescence spectra of different tissue types, for both perpendicular and parallel polarizations are subjected to a five level DWT decomposition.

After DWT, what we obtain are the coefficients

$d_{j,k}$'s (also called high-pass coefficients) at levels 1

through 5. As was mentioned earlier, in the Haar basis, the level-1 coefficients are the differences of the nearest neighbour fluorescence spectral intensities multiplied by a factor of $1/\sqrt{2}$. For an N-size data set, one level decomposition results in N/2 number of high pass coefficients and also the same number of low pass coefficients. At the next level of decomposition, the coefficients are the differences of the nearest neighbour averages, multiplied by 1/2, resulting in N/4 coefficients. Hence, at each level of decomposition, the number of the resulting coefficients is half that of the parent set from which they are computed. The wavelet decomposition of fluorescence spectra of normal as well as cancerous tissue is shown in figures 1 and 2 respectively. It is to be noted that the wavelet decomposition of the intensity spectral profile alone is not sufficient to differentiate the tissue type. These coefficients now constitute the feature vectors for further statistical analysis; in this case the LDA for the purpose of classification.

This paper develops rules for classification of tissue, using Discriminant Analysis, into three classes (Normal, Malignant or Benign) based on all the features which are the detail wavelet coefficients at specified levels 3,4,5. The results of such an analysis are presented in figures 3 to 5. The first two levels of wavelet coefficients contain variations at high resolution and the statistical nature of these fluctuations has been analysed in earlier studies [14]. Variations at a higher level, for example from level 3 onwards are a result of certain amount of averaging and hence are less prone to statistical or instrumental uncertainties. Furthermore they are expected to carry signatures of the tissue type, since the characteristic spectral variations in different type of tissues show variations over a broader range of wavelengths. This is the reason for doing the present analysis on the coefficients from level 3 onwards. Considering the length of the data for each patient (~200), going further up in the decomposition beyond level 5 is not advisable as the wavelet coefficients at the end points would be affected either by padding or circular extension. The three score functions are obtained with the help of STATISTICA for each of the data obtained from 29 normal (N) tissues, 18 malignant tissues (M) and 11 benign tissues (B) giving rise to a total of 58 X 3 of the same. Out of these three scores corresponding to a given patient, two distances can be computed, which are the differences of the three score functions. For example, M-N gives the difference of the scores corresponding to Malignant and Normal. The quantity M-N being positive, implies that the sample is closer to normal rather than malignant; hence it can be inferred that the corresponding tissue is normal. Scatter plots are obtained for the differences of scores N-B vs M-N, M-N vs B-M and B-M vs N-B with appropriate legend for the points based on the tissue type in Figures 3 to 5 for levels 3, 4 and 5 respectively. The region in the north-west corner refers to the classification to Normal in (a), Malignant in (b) and Benign in (c). From a count of the points in the north-west region, the table in fig_(d) is obtained which gives the power of classification in this study, which is carried out using the discriminant function of the features namely the wavelet

detail coefficients at a given level. The results of the sensitivity of the classification for each level are shown in the following table.

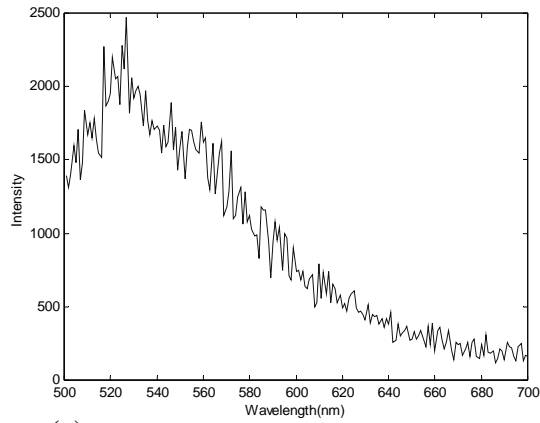
level	BENIGN	MALIGNANT	NORMAL	Total
3	73	89	86	85
4	64	78	83	78
5	64	61	69	66

One can observe that as the level increases, the dimension of the feature space decreases and hence the sensitivity decreases which shows that there is a trade off between the dimension and sensitivity. Depending upon the information that is sought, one needs to pick up the appropriate level. The analysis carried above is for the perpendicularly polarized spectra and the same steps have been repeated for the case of parallel polarization and the results for this case show comparable accuracy.

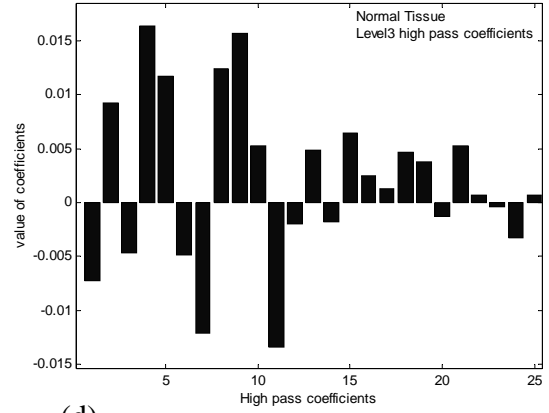
VI. CONCLUSION

In conclusion, from the discrete wavelet transform of parallel and perpendicular polarized spectra of cancerous and normal tissues, several local and global parameters have been identified distinguishing normal tissue from the cancerous counterparts. Detail wavelet coefficients have been used in the analysis because of the fact that wavelet decomposition upto a particular level results in a DC (Constant) value (at coarser level) and fluctuations above this DC component at other levels which information is present in the detail coefficients. Detail wavelet coefficients have shown an optimistic trend in classification of tissue spectra.

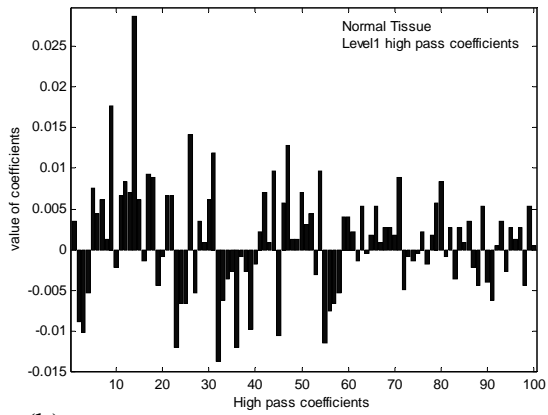
In this paper, discriminant analysis has been applied only on the high pass coefficients at a particular level wherein no specific algorithm has been used for feature selection. Therefore further work can be carried out on feature selection considering all levels of high pass coefficients and also the wavelet packet decomposition. For this purpose, machine-learning algorithms such as neural networks may be more suitable.



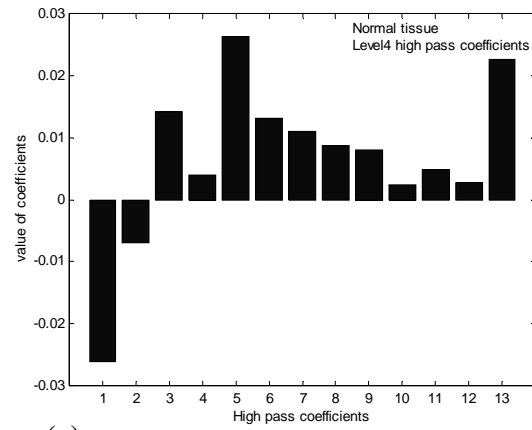
(a)



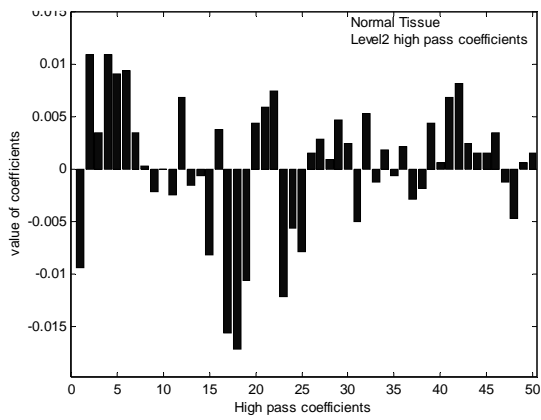
(d)



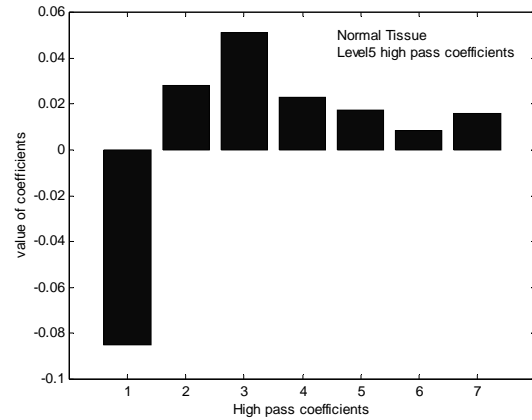
(b)



(e)

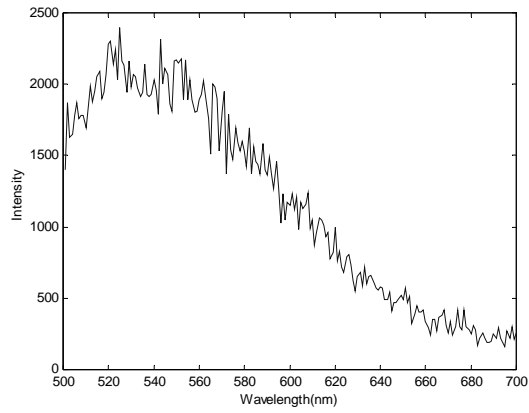


(c)

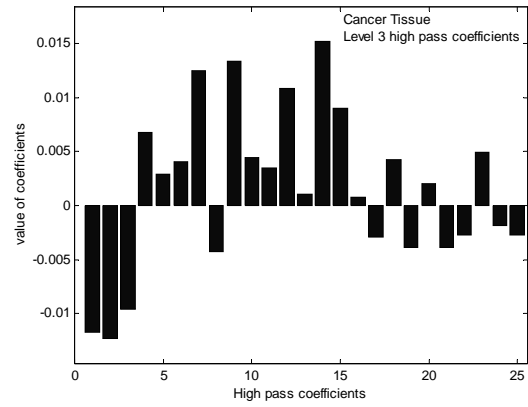


(f)

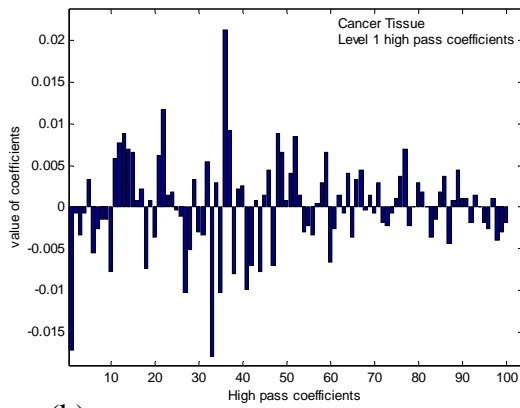
Fig. 1. (a) Fluorescence spectrum of a normal tissue, whose (high-pass) wavelet coefficients at different levels are displayed in (b) level-1, (c) level-2, (d) level-3, (e) level-4, and (f) level-5



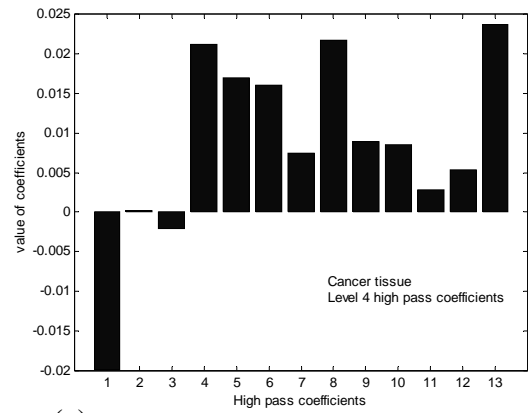
(a)



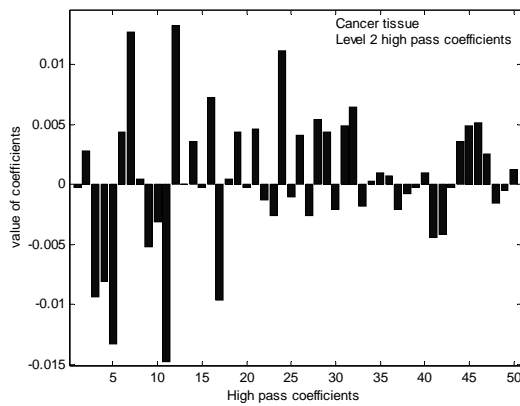
(d)



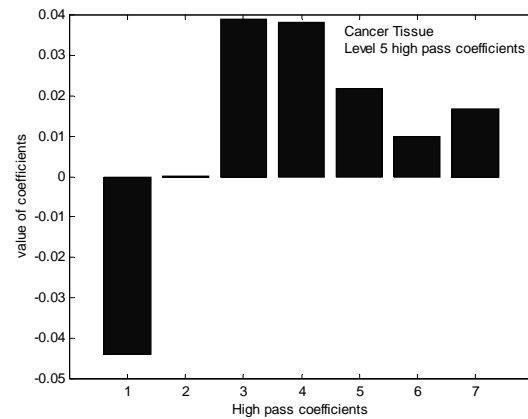
(b)



(e)

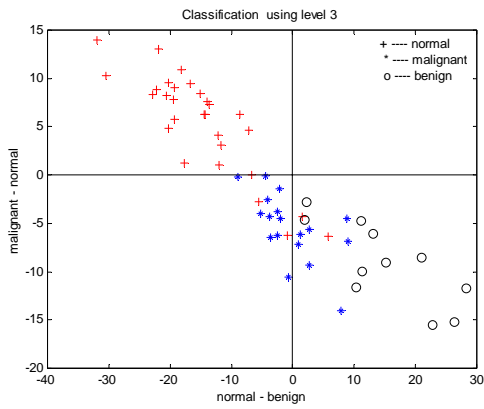


(c)

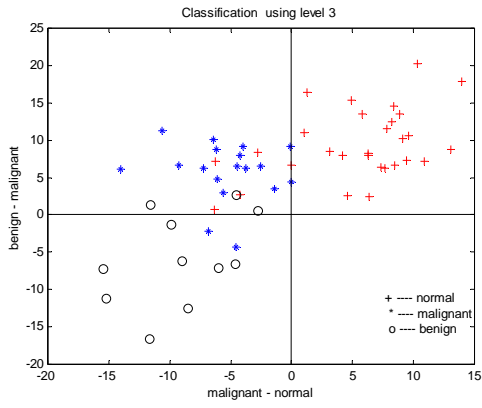


(f)

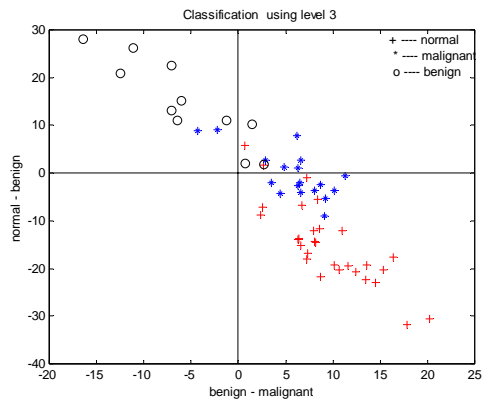
Fig. 2. (a) Fluorescence spectrum of a cancerous tissue, whose wavelet (high-pass) coefficients at different levels are displayed in (b) level-1, (c) level-2, (d) level-3, (e) level-4 and (f) level-5



(a)



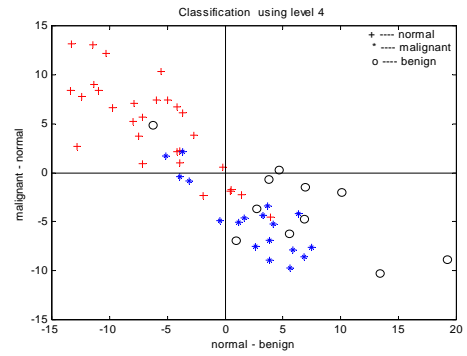
(b)



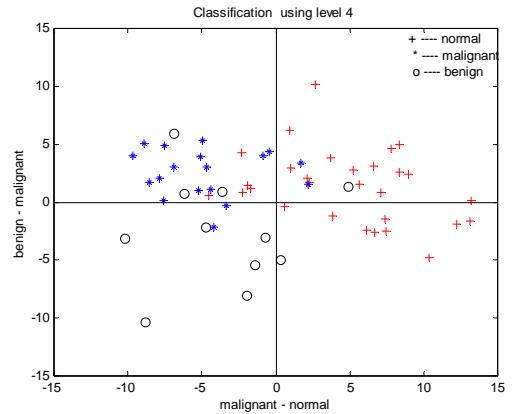
(c)

Classification Matrix (level3) Rows: Observed classifications Columns: Predicted classifications				
type	sensitivity	NORMAL	MALIGNANT	BENIGN
NORMAL	86	25	4	0
MALIGNANT	89	0	16	2
BENIGN	73	0	3	8
Total	85	25	23	10

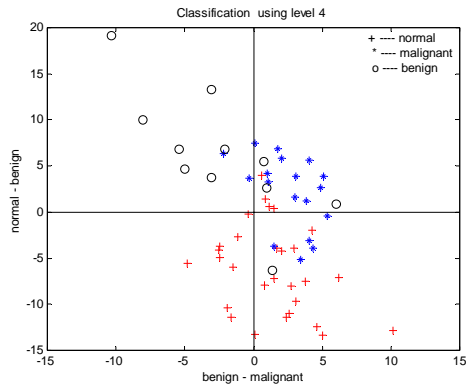
(d)



(a)



(b)



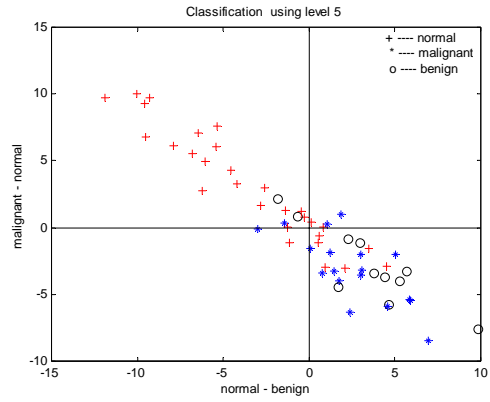
(c)

Classification Matrix (level4) Rows: Observed classifications Columns: Predicted classifications				
type	sensitivity	NORMAL	MALIGNANT	BENIGN
NORMAL	83	24	5	0
MALIGNANT	78	2	14	2
BENIGN	64	1	3	7
Total	78	27	22	9

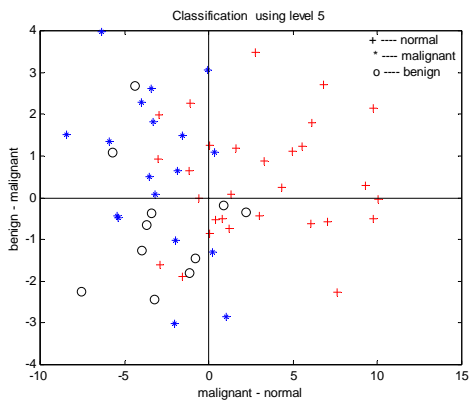
(d)

Fig. 3. First quadrant represents the region (a)Normal, (b)Malignant, (c) benign, and (d) represents the classification matrix for level 3

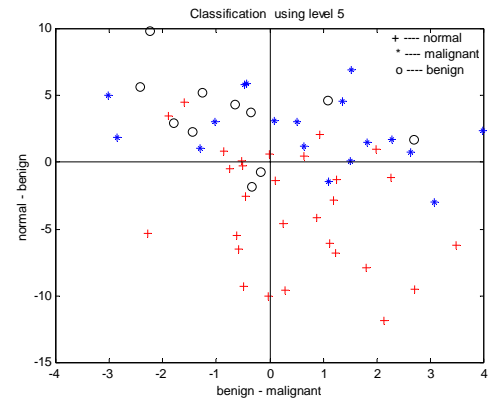
Fig. 4. First quadrant represents the region (a)Normal, (b)Malignant, (c) benign, and (d) represents the classification matrix for level 4



(a)



(b)



(c)

Classification Matrix (level 5) Rows: Observed classifications Columns: Predicted classifications				
type	sensitivity	NORMAL	MALIGNANT	BENIGN
NORMAL	69	20	4	5
MALIGNANT	61	1	11	6
BENIGN	64	2	2	7
Total	66	23	17	18

(d)

Fig. 5. First quadrant represents the region (a)Normal, (b)Malignant, (c) benign, and (d) represents the classification matrix for level 4

REFERENCES

- [1] R. R Alfano, B. B. Das, J. Cleary, R. Prudente and E. Celmer, "Light sheds light on cancer distinguishing malignant tumors from benign tissues and tumors," Bull. NY Acad. Med., 2nd Series, vol. 67, 1991, pp. 143-150.
- [2] For recent progress in this area see IEEE J. Quantum Electron., vol. 9, 2003, pp. 140-343.
- [3] R. R Alfano, D. Tata, J. Cordero, P. Tomashefsky, F.Longo, and M. A. Alfano, "Laser induced fluorescence spectroscopy from native cancerous and normal tissues," IEEE J. Quantum Electron., vol. QE-20, 1984, pp. 1507-1511.
- [4] R. R Alfano, G. C. Tang, A. Pradhan, W. Lam, D. S. J. Choy, and E. Opher, "Fluorescence spectra from malignant and normal human breast and lung tissues," IEEE J. Quantum Electron., vol. QE-23, 2003, pp. 1806.
- [5] D. B. Tata, M. Foresti, J. Cordero, P. Tomashefsky, M. Alfano, and R. R. Alfano, "Fluorescence polarization spectroscopy and time resolved fluorescence kinetics of native cancerous and normal rat kidney tissues," Biophys. J., vol. 50, 1986, pp. 463-469.
- [6] N. Ramanujam, M. F. Mitchell, A. Mahadevan-Jansen, S. Thomsen, G. Staerckel, A. Malpica, T. Wright, A. Atkinson, and R. Richards – Kortum, "Cervical pre-cancerous detection using a multivariate statistical algorithm based on laser induced fluorescence spectra at multiple excitation wavelengths," Photochem. Photobiol., volk 64, 1996, pp. 720-735.
- [7] R. W. Dillon and M. Goldstein, Multivariate Interpretation of Clinical Laboratory Data. New York: Marcel Dekker, 1987.
- [8] F. N. Ghadially, W. J. P. Neish, and H. C. Dawkins, "Mechanism involved in the production of red fluorescence of human and experimental tumors," J. Pathol. Bacteriol., vol. 85, 1963, pp. 77-92; J. Wu, M. S. Feld and R. P. Rava, "Analytical model for extracting intrinsic fluorescence from a turbid media," Appl. Opt., vol 32, 1993, pp. 3585-3595.
- [9] I. Daubechies, Ten Lectures on Wavelets. Philadelphia, PA: Society for Industrial and Applied Mathematics, vol. 64, 1992, CBMS-NSF Regional Conference Series in Applied Mathematics.
- [10] D. Donoho, I. Johnstone, G. Kerkyacharian, and D. Pichard, "Wavelet shrinkage: Asymptopia?," J. Roy. Statist. Soc., vol. 57, 1995, pp. 301-369.
- [11] Donoho, I. Johnstone, "Minimax Estimation via Wavelet Shrinkage", Anal. of Statist., vol. 26, 1998, pp. 879-921.
- [12] D. Donoho, I. Johnstone, "Ideal Spatial Adaptation by Wavelet shrinkage", Biometrika., vol. 81, pp. 1994. 425-553.
- [13] Richard O.Duda, Peter E. Hart Devid G. Stork, "Pattern Classification", John Wiley & Sons Inc, 2000. pp. 215-286.
- [14] Nidhi Agarwal, Sharad Gupta, Bhawna, Asima Pradhan, K. Vishwanathan, and Prasanta K. Panigrahi, "Wavelet Transform of Breast Tissue Fluorescence Spectra: A Technique for Diagnosis of Tumors ", IEEE J. Quantum Electron., Vol. 9, 2003, pp. 154-161.
- [15] Yahen Wang, "Jump and Sharp Cups detection by Wavelets", Biometrika , vol 82, 1995, pp. 385-397.
- [16] Richard A. Johnson, Dean W. Wichern, "Applied Multivariate Statistical Analysis", Prentice-Hall of India, 2001, pp. 493-600.
- [17] B. V. Laxmi, R. N. Panda, M. S. Nair, A. Rastogi, D. K. Mittal, A. Agarwal, and A. Pradhan, "Distinguishing normal, benign and malignant human breast tissues by visible polarized fluorescence," Lasers Life Sci., vol. 9, 2001, pp. 229-243.
- [18] M. S. Nair, N. Ghosh, N. S. Raju, and A. Pradhan, "Propagation of fluorescence in human breast tissues: A diffusion theory model," Appl. Opt., vol. 41, no. 19, 2002, pp. 4024-4035.

Bhadra Mani received the M.Sc. degree from Indian Institute of Technology (IIT), Delhi, India, and done the M.Tech.[Comp. Tech] from University of Hyderabad.

C. Raghavendra Rao received Ph.D (Statistics) and M.Tech (CSE) from the Osmania University, Hyderabad in 1986 and 1999 respectively. He is a Member of the Faculty at the School of MCIS University of Hyderabad, India since 1986. His current research interests include Operation Research, Simulation & Modeling, Knowledge Discovery, Rough Sets, Neural Networks, Pattern Recognition, Data mining, Wavelet Transforms and Computer Based Optimization. Dr C. R. Rao is a member of the Operation Research Society of India, Indian Mathematical Society and a Fellow of IETE and a member of IAENG (Membership number 61460).

P. Anantha Lakshmi received the Ph.D. degree from the University of Hyderabad, Hyderabad. She is a member of the faculty at the School of Physics, University of Hyderabad. Her research interests include Quantum Optics, Nonlinear Optics, Application of wavelet transforms.

Asima Pradhan received the Ph.D. degree from the Center for Ultrafast Spectroscopy and Lasers, City College of New York (CUNY), in 1991. She has been working in the field of biomedical optics for the past several years. She now works on light propagation in turbid media using lasers and noninvasive diagnosis of tumors at IIT Kanpur

Prasanta K. Panigrahi received the Doctoral degree from the University of Rochester, Rochester, NY, in 1988. He was a Member of the Faculty at the University of Hyderabad. He has now joined the Quantum Optics and Quantum Information Group, Physical Research Laboratory, Ahmedabad, India. Currently, his interests include Bose Einstein Condensation, Wavelet Transform, and Quantum Computation.